Diffraction pattern from thermal neutron incoherent elastic scattering and the holographic reconstruction of the coherent scattering length distribution

B. Sur,[1] V. N. P. Anghel,[1] R. B. Rogge,[2] and J. Katsaras[2]
[1]*Atomic Energy of Canada Limited, Chalk River Laboratories, Chalk River, Ontario, K0J 1J0, Canada*
[2]*Steacie Institute for Molecular Sciences, National Research Council, Chalk River, Ontario, K0J 1J0, Canada*
(Received 23 October 2003; revised manuscript received 28 May 2004; published 6 January 2005)

The diffraction of spherical waves (*S* waves) interacting with a periodic scattering length distribution produces characteristic intensity patterns known as Kossel and Kikuchi lines (collectively called *K* lines). The *K*-line signal can be inverted to give the three-dimensional structure of the coherent scattering length distribution surrounding the source of *S* waves—a process known as "Gabor holography" or, simply, "holography." This paper outlines a kinematical formulation for the diffraction pattern of monochromatic plane waves scattering from a mixed incoherent and coherent *S*-wave scattering length distribution. The formulation demonstrates that the diffraction pattern of plane waves incident on a sample with a uniformly random distribution of incoherent scatterers is the same as that from a sample with a single incoherent scatterer per unit cell. In practice, one can therefore reconstruct the holographic data from samples with numerous incoherent *S*-wave scatterers per unit cell. Thus atomic resolution thermal neutron holography is possible for materials naturally rich in incoherent thermal neutron scatterers, such as hydrogen (e.g., biological and polymeric materials). Additionally, holographic inversions from single-wavelength data have suffered from the so-called conjugate or twin-image problem. The formulation presented for holographic inversion—different from those used previously [e.g., T. Gog *et al.*, Phys. Rev. Lett. **76**, 3132 (1996)]—eliminates the twin-image problem for single-wavelength data.

DOI: 10.1103/PhysRevB.71.014105 PACS number(s): 61.12.Ex

I. INTRODUCTION

In the Born approximation, the interaction of single-frequency plane waves with a three-dimensional (3D) periodic scattering length distribution produces diffraction maxima in discrete directions (i.e., Bragg peaks). Similarly, single-frequency spherical waves (*S* waves) interacting with a periodic 3D scattering length distribution (e.g., atoms on a lattice) give rise to sharp intensity variations in conical directions; the conic sections are referred to as *K* lines.[1] *K* lines resulting from *S* waves created by electronic deexcitations (e.g., photoemission or fluorescence) of atoms inside the crystal sample are commonly referred to as Kossel lines,[2,3] while those generated by dynamical effects (e.g., inelastic or multiple scattering) are typically called Kikuchi lines.[4] The line structure of Kossel lines was predicted in 1922 by Clark and Duane[2] and experimentally observed using x rays and a single crystal of copper by Kossel, Loeck, and Voges[3] in 1934. Kikuchi lines were first observed in electron scattering studies of varying thickness mica plates.[4]

The *K*-line intensity pattern depends on the relative position of the periodic scatterers with respect to the spherical wave source—i.e., the crystallographic phase of the scattering structure function. Thus *K* lines provide the signal for direct three-dimensional, atomic resolution imaging techniques (holography) for single crystals via the so-called "inside source"[5,6] or "inside detector" concept.[7] In the case of inside source holography, the detected interference pattern (hologram) is viewed as being formed by *S* waves emitted by atoms inside the sample, while in the case of inside detector holography the integrated diffraction intensity is interpreted as atoms inside the sample detecting the interference field. In either case, an *S*-wave atomic resolution hologram is the result of a uniform spherical reference wave interfering with a nonuniform object wave.

Unlike electrons and x rays, neutrons scatter from atomic nuclei which for thermal neutron waves act as point or pure *S*-wave scatterers. *K* lines are a fundamental feature of monochromatic *S*-wave diffraction by a periodic scattering length distribution. Until recently, *K* lines had never been identified in experimental thermal neutron scattering data although their presence had been predicted theoretically, for both incoherent elastic scattering[8] and dynamical scattering.[9] The first observation of *K* lines using thermal neutrons was made by Sur *et al.*[1] using a single crystal of potassium dihydrogen phosphate (KDP), a sample containing strong incoherent scatterers. This experimental observation suggests that thermal neutron atomic structure holography is feasible.

The beginnings of atomic resolution holography can be traced to Bragg's x-ray work[10] and Gabor's electron interference microscope.[11] Although Gabor's lensless microscope was not realized in his lifetime, over the past decade or so there has been an increasing number of publications on atomic resolution holography using either electrons[12–15] or hard x rays.[7,16–19] More recently, Sur *et al.* demonstrated experimentally the feasibility of atomic resolution thermal neutron holography using a single crystal containing one *S*-wave incoherent scatterer (H atom) per unit cell.[20] In that experiment neutron holography was demonstrated via the inside source concept. Subsequently, neutron holography using the inside detector concept was carried out by recording the hologram of lead nuclei in a Pb(Cd) single crystal.[21]

Although the above-mentioned studies employed single-crystal samples this is not necessary. For atomic structure

holography the only requirement is that the sample possess orientational order, translational order is not a necessary condition. A good source of neutron *S* waves is hydrogen atoms which possess a large incoherent neutron scattering cross section: $\sigma_i = 80$ b. Because biomimetic and polymeric materials are typically rich in hydrogen, contain other low-*Z* atoms, and often possess only orientational order, they are expected to be particularly well suited to thermal neutron holography.

Until now the mathematical formulations for atomic structure holography have been limited to samples with one *S*-wave source per unit cell. Starting from this point (Sec. II), we develop formulations for the diffraction pattern of extended coherent and incoherent *S*-wave sources (Sec. III). This leads to a second-order kinematical formulation of plane-wave scattering from a mixed coherent and incoherent *S*-wave scattering length distribution (Sec. IV), from which it becomes evident that one can reconstruct the atomic structure of samples with a uniformly random distribution of incoherent scatterers. In practice, for thermal neutron holography, this condition can be achieved by samples with a large number of hydrogen atoms per unit cell. Finally, we give a formulation for holographic reconstruction that eliminates the twin-image problem from single-wavelength data (Sec. V).

II. DIFFRACTION PATTERN OF *S* WAVES FROM A SINGLE-POINT SOURCE

Consider a point source at the origin, producing spherical waves with wave number k and amplitude a. Omitting the time dependence, the unperturbed or reference wave displacement at position $\mathbf{r}$ is given by

$$\Psi_{ref}(\mathbf{r}) = a\frac{e^{ik|\mathbf{r}|}}{|\mathbf{r}|}. \tag{1}$$

If the source is surrounded by a distribution of weak, point, or pure *S*-wave elastic scatterers, characterized by a scattering length density $b(\mathbf{r})$, then in the Born approximation the scattered or object wave is

$$\Psi_{obj}(\mathbf{r}) = a\int_{\mathbf{r}_0}\frac{b(\mathbf{r}_0)e^{ik(|\mathbf{r}_0|+|\mathbf{r}-\mathbf{r}_0|)}}{|\mathbf{r}_0||\mathbf{r}-\mathbf{r}_0|}d\mathbf{r}_0. \tag{2}$$

The total wave amplitude for a detector at a distance $\mathbf{R}$ is equal to $\Psi_{ref}(\mathbf{R})+\Psi_{obj}(\mathbf{R})$. The detected intensity $I_{1s}(\mathbf{R})$ can then be written as $[\Psi^*_{ref}\Psi_{ref}+2\,\mathrm{Re}(\Psi^*_{ref}\Psi_{obj})+\Psi^*_{obj}\Psi_{obj}]$. In the far field $R \gg r$ and defining the outgoing wave vector in the direction of the detector as $\mathbf{k}_{out} \equiv k\hat{\mathbf{R}}$, we can write the detected intensity as

$$I_{1s}(\mathbf{k}_{out}) \cong \frac{a^* a}{R^2}[1 + 2\,Re[\chi(\mathbf{k}_{out})] + |\chi(\mathbf{k}_{out})|^2], \tag{3}$$

where the intensity modulation function is

$$\chi(\mathbf{k}_{out}) = \int\frac{b(\mathbf{r}_0)e^{i(kr_0-\mathbf{k}_{out}\cdot\mathbf{r}_0)}}{r_0}d\mathbf{r}_0, \tag{4}$$

as derived in Appendix A.

In Eq. (3), the first term is the unperturbed constant reference-wave intensity due to the source. The object causes a modulation of this reference intensity as described by the second and third terms in Eq. (3). Holographic imaging of the object scattering length distribution via the inside source concept is essentially the Fourier inversion of the intensity modulation.

By defining a Fourier transform

$$B(\mathbf{q}) = \frac{1}{\sqrt{(2\pi)^3}}\int b(\mathbf{r})e^{-i\mathbf{q}\cdot\mathbf{r}}d\mathbf{r}, \tag{5}$$

the modulation function in reciprocal space is

$$\chi(\mathbf{k}_{out}) = \frac{4\pi}{\sqrt{(2\pi)^3}}\int\frac{B(\mathbf{q})}{|\mathbf{q}|^2 - 2\mathbf{k}_{out}\cdot\mathbf{q}}d\mathbf{q}. \tag{6}$$

A periodic three-dimensional scattering length distribution is completely described by the magnitude and phase of its structure function F_{hkl} at discrete points in reciprocal space. The reciprocal-lattice points are given by $\boldsymbol{\tau}_{hkl} = h\mathbf{b}_1 + k\mathbf{b}_2 + l\mathbf{b}_3$ where $\mathbf{b}_1$, $\mathbf{b}_2$, and $\mathbf{b}_3$ are three reciprocal-lattice basis vectors. Equation (5) can thus be written as a series—i.e.,

$$B(\mathbf{q}) = \sum_{hkl} F_{hkl}\delta(\mathbf{q} - \boldsymbol{\tau}_{hkl}). \tag{7}$$

Thus, for a periodic scattering length distribution Eq. (6) becomes a sum over all *hkl*—namely,

$$\chi(\mathbf{k}_{out}) = \frac{4\pi}{\sqrt{(2\pi)^3}}\sum_{hkl}\frac{F_{hkl}}{|\boldsymbol{\tau}_{hkl}|^2 - 2\mathbf{k}_{out}\cdot\boldsymbol{\tau}_{hkl}}. \tag{8}$$

For every pair of discrete points, $\pm\boldsymbol{\tau}_{hkl}$ located within a sphere of radius $2k$, the zeros in the denominator of Eq. (8) cause the modulation to go to infinity in $\mathbf{k}_{out}$ directions whose locus is a cone with axis along $\pm\boldsymbol{\tau}_{hkl}$ and full opening angle 2θ satisfying the relation $2k\cos\theta = \tau_{hkl}$. The intersection of the cone with a surface is a *K* line. The intensity modulation due to the second term in Eq. (3) changes sign on crossing the *K* line. In comparison, the third term in Eq. (3) is always positive, relatively narrow, and just sufficient to ensure that the total modulation never becomes negative (unphysical). The derivations in this section are valid only for a single source of monochromatic *S* waves located inside an object.

III. DIFFRACTION OF *S* WAVES FROM EXTENDED SOURCES

We consider two cases of an extended source: a continuous or coherent source and a distribution of independent or incoherent sources. The formulation in Sec. II can be extended to the case of multiple sources by describing a continuous or coherent source in real space as a complex amplitude density $a(\mathbf{r})$ [$A(\mathbf{q})$ in reciprocal space]. As shown in Appendix B, the intensity detected in the far field $[\Psi^*_{ref}\Psi_{ref}+2\,\mathrm{Re}(\Psi^*_{ref}\Psi_{obj})+\Psi^*_{obj}\Psi_{obj}]$ can be expressed as follows:

$$I_{ns}(\mathbf{k}_{out}) \cong \frac{1}{R^2}[A * A + 2\,\mathrm{Re}(A * \tilde{B}) + |\tilde{B}|^2], \tag{9}$$

where

$$\tilde{B}(\mathbf{k}_{out}) = 4\pi \int \frac{A(\mathbf{k}_{out} - \mathbf{q})B(\mathbf{q})}{|\mathbf{q}|^2 - 2\mathbf{k}_{out}\cdot\mathbf{q}} d\mathbf{q}. \tag{10}$$

A comparison of Eqs. (9) and (10) with Eqs. (3)–(8) readily shows that if $b(\mathbf{r})$ is periodic, one would again expect to see K lines for an extended coherent source. The K-line modulation for the case of an extended coherent source [Eq. (10)] depends on both the structure of the source and of the object.

Similarly, the formulation in Sec. II can be extended to a distribution of independent or incoherent sources. A distribution of point S-wave sources uncorrelated in time implies that the phase (but not necessarily the magnitude) of $a(\mathbf{r})$ is uniformly random as a function of $\mathbf{r}$. For this case, by defining $A^2(\mathbf{q})$ as the Fourier transform of $|a(\mathbf{r})|^2$, the three terms for the intensity detected in the far field, as shown in Appendix C, are

$$\psi^*_{ref}(\mathbf{k}_{out})\psi_{ref}(\mathbf{k}_{out}) = A^2(0), \tag{11}$$

$$\psi^*_{ref}(\mathbf{k}_{out})\psi_{obj}(\mathbf{k}_{out}) + \text{c.c.} = 2\,\mathrm{Re}\left[\int \frac{4\pi A^2(-\mathbf{q})B(\mathbf{q})}{|\mathbf{q}|^2 - 2\mathbf{k}_{out}\cdot\mathbf{q}} d\mathbf{q}\right], \tag{12}$$

$$\psi^*_{obj}(\mathbf{k}_{out})\psi_{obj}(\mathbf{k}_{out}) = A^2(0)\left|\int \frac{4\pi B(\mathbf{q})}{|\mathbf{q}|^2 - 2\mathbf{k}_{out}\cdot\mathbf{q}} d\mathbf{q}\right|^2. \tag{13}$$

The first term $A^2(0)$ is the uniform, total (incoherent) unperturbed intensity due to the source distribution. The third term gives a positive K-line modulation that depends only on the magnitude and not the phase of the scattering length distribution. For a source and scattering length distribution with the same periodicity (inside source), the interference between the reference and object waves—i.e., Eq. (12)—gives a K-line modulation similar to Eq. (8), which depends on the relative position—i.e., the phase of the scatterers with respect to the sources. For a single fixed point source per period or for a uniformly random (spatially incoherent or perfectly diffuse) source, $A^2(\mathbf{q}) = A^2(\boldsymbol{\tau}_{hkl}) = A^2(0)$, and the distributed independent source K-line expressions [Eqs. (11)–(13)] reduce exactly to the single-point-source case [Eqs. (3)–(8)]. The observed diffraction pattern (i.e., hologram) for both these cases can be inverted to give the scattering length distribution (i.e., atomic structure) of the object. Atomic structure holography with a uniformly random source distribution is analogous to the commonly used diffuser in optical holography.

IV. DIFFRACTION OF PLANE WAVES BY A MIXED COHERENT AND INCOHERENT SCATTERING LENGTH DISTRIBUTION

For plane waves interacting with a periodic scattering length distribution, the Born (single scattering) approximation does not give rise to K lines. Consider, however, the elastic scattering diffraction pattern in the far field due to the interference between the first scattered wave, Ψ_I, and a subsequent second scattered wave, Ψ_{II}, as depicted in Fig. 1. The detected intensity (evaluated for incident and detected wave vectors $\mathbf{k}_{in}$ and $\mathbf{k}_{out}$) is given by the expression,

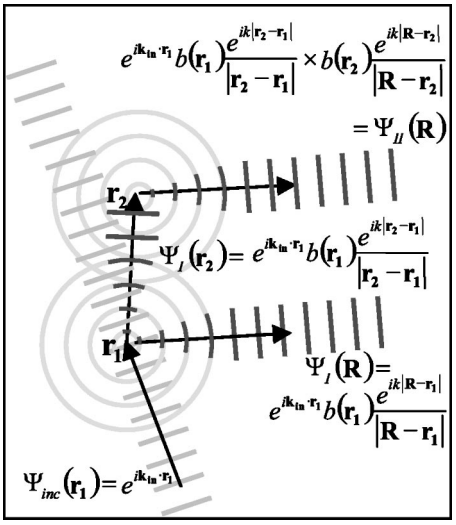

FIG. 1. Schematic depiction of second-order plane-wave scattering. The incident neutron plane wave Ψ_{inc} interacts with an atom at $\mathbf{r}_1$ producing a primary spherical wave Ψ_1. This primary S wave interacts with a second atom at $\mathbf{r}_2$, producing a secondary S wave Ψ_{II}. The interference between the primary and secondary S waves leads to an intensity modulation detected at $\mathbf{R}$.

$$I(\mathbf{k}_{in}, \mathbf{k}_{out}) = \Psi^*_I\Psi_I + 2\,\mathrm{Re}(\Psi^*_I\Psi_{II}) + \Psi^*_{II}\Psi_{II}. \tag{14}$$

Consideration of the second-order scattering process leads to a complete stationary solution to the wave equation, which is a second-order partial differential equation. Consider the scattering length distribution as the sum of a time-invariant, perfectly periodic, coherent component $b_c(\mathbf{r})$ [$B_c(\mathbf{q})$ in reciprocal space] and a uniformly random, incoherent component with squared-magnitude $|b_i(\mathbf{r})|^2$ [$B_i^2(\mathbf{q})$ in reciprocal space]. As shown in detail in Appendix D, the detected intensity [Eq. (14)] separates into two contributions. One is from purely coherent scattering, while the other is from the interaction between coherent and incoherent scattering. The purely coherent contribution is given by

$$I_{coh}(\mathbf{k}_{in}, \mathbf{k}_{out}) \cong \frac{1}{R^2}(B^*_cB_c + 2\,\mathrm{Re}(B^*_c\tilde{B}_c) + |\tilde{B}_c|^2). \tag{15}$$

In Eq. (15), B_c is evaluated at $\boldsymbol{\kappa} = \mathbf{k}_{out} - \mathbf{k}_{in}$ and

$$\tilde{B}_c(\mathbf{k}_{in}, \mathbf{k}_{out}) = 4\pi \int \frac{B_c(\boldsymbol{\kappa} - \mathbf{q})B_c(\mathbf{q})}{|\mathbf{q}|^2 - 2\mathbf{k}_{out}\cdot\mathbf{q}} d\mathbf{q}. \tag{16}$$

The first term in Eq. (15) is the Born approximation and leads to Bragg maxima at $\boldsymbol{\kappa} = \boldsymbol{\tau}_{hkl}$. For the case of elastic scattering, the second and third terms in Eq. (15) are implicitly symmetrical in $\mathbf{k}_{out}$ and $-\mathbf{k}_{in}$. These terms lead to a

modulation of the Bragg peak intensity of a particular $\boldsymbol{\tau}_{hkl}$, when scanned as a function of $\mathbf{k}_{out}$ and $-\mathbf{k}_{in}$ (e.g., Pendellösung fringes).

The detected intensity from the interaction of the incoherent and coherent scattering naturally separates into contributions depending separately on $\mathbf{k}_{out}$ and $-\mathbf{k}_{in}$. It is shown in Appendix D that these two contribution can each be cast in the same form as Eqs. (11)–(13).

Monochromatic plane-wave incoherent scattering thus gives the same *K*-line pattern as a distribution of monochromatic, independent sources for scans in both the sample-to-detector and beam-to-sample directions. So-called inside source data are obtained by scanning $\mathbf{k}_{out}$ directions only, while inside detector data are obtained by scanning $\mathbf{k}_{in}$ directions only. The hologram has a $\boldsymbol{\kappa}$ dependence when the incoherent scattering distribution is nonuniform.

The *K*-line intensity profile, as predicted by the kinematical formulation of internal source and of plane-wave incoherent elastic scattering from a periodic scattering length distribution, is broadened by both the experimental arrangement and the scattering length distribution. Examples of factors leading to *K*-line broadening are the following.

(i) Finite sample shape leads to a convolution of the modulation $\chi(\mathbf{k})$ with a shape function.

(ii) Dynamics or "internal structure" or higher-order partial-wave scattering in the periodic coherent scatterers $b_c(\mathbf{r})$ causes broadening of the structure function $B_c(\boldsymbol{\tau}_{hkl})$ at each reciprocal lattice point.

(iii) Motion of the scatterers leads to a nonuniform reference wave intensity $B_i^2(\boldsymbol{\kappa})$.

(iv) Finite $\Delta\lambda/\lambda$ of the incident beam wavelength results in the convolution of $\chi(\mathbf{k})$ with the wavelength spread function.

(v) Angular spread of the incident beam and finite detector angular resolution leads to a convolution $\chi(\mathbf{k})$ with the angular resolution function.

We have calculated an analytical solution for the shape of *K* lines when the "ideal" modulation function is convoluted with a generic Gaussian spread function. The derivation, in its entirety, and the solution to this problem are presented in Appendix E.

V. RECONSTRUCTION OF THE COHERENT SCATTERING LENGTH DISTRIBUTION FROM THE *S*-WAVE DIFFRACTION PATTERN

The above considerations show that the diffraction pattern of single-frequency spherical waves produced by incoherent scattering contains both amplitude and phase information for all of reciprocal space within a radius of $2k$, where k is the wave-vector magnitude. Holographic reconstruction is possible because for a distribution of weak scatterers the diffraction pattern is dominated by a linear rather than a quadratic dependence on the coherent scattering length distribution. As well, it was shown in Sec. III that the diffraction pattern of waves from a single-point spherical wave source has the same form as that from a uniformly random source distribution. This equivalence is commonly exploited in optical holography with a diffuse source. In the case of neutron scattering, both these conditions (i.e., relatively strong and uniformly random incoherent scatterers) are readily satisfied by biological or polymeric materials which typically contain many hydrogen atoms, a relatively strong incoherent scatterer.

As per Eqs. (3) and (4) and Eqs. (11)–(13), the experimentally observed hologram modulation function $H(\mathbf{k})$ produced by the interaction of a weak *S*-wave coherent scattering length distribution $b(\mathbf{r})$ with either a single incoherent point scatterer or with a uniform distribution of incoherent scatterers is given, aside from constants, by

$$H(\mathbf{k}) \sim \int \mathrm{Re}\left[\frac{b(\mathbf{r})}{r} e^{[i(kr-\mathbf{k}\cdot\mathbf{r})]}\right] d\mathbf{r} + O(b^2). \tag{17}$$

The conditions for pure *S*-wave, weak scattering are particularly well satisfied for unpolarized thermal neutron scattering from nuclei. Additionally, for most nuclei, the thermal neutron coherent scattering lengths are almost purely real and have the same sign. The real part of the coherent scattering length distribution can be directly reconstructed from the measured hologram modulation function using the following relations:

$$\tilde{b}_{even}(\mathbf{r}) = \frac{b_{real}(\mathbf{r}) + b_{real}(-\mathbf{r})}{kr}\cos(kr)$$

$$\propto \int_{constant\ |\mathbf{k}|} H(\mathbf{k})\cos(\mathbf{k}\cdot\mathbf{r})d\mathbf{k} \tag{18}$$

and

$$\tilde{b}_{odd}(\mathbf{r}) = \frac{b_{real}(\mathbf{r}) - b_{real}(-\mathbf{r})}{kr}\sin(kr)$$

$$\propto \int_{constant\ |\mathbf{k}|} H(\mathbf{k})\sin(\mathbf{k}\cdot\mathbf{r})d\mathbf{k}. \tag{19}$$

Strictly speaking, for a single wavelength or constant k, the even and odd parts are reconstructed at nonoverlapping points in space (i.e., the zeros of the even part reconstruct at turning points of the odd part and vice versa). As such, it is possible to eliminate the conjugate image $b_{real}(-\mathbf{r})$ from the reconstruction of a single-hologram data set by a suitable combination of $\tilde{b}_{odd}(\mathbf{r})$ and $\tilde{b}_{even}(\mathbf{r})$. For instance, $\tilde{b}_{odd}(\mathbf{r})\sin(kr)$ and $\tilde{b}_{even}(\mathbf{r})\cos(kr)$ can be summed with a moving box average of dimensions $\lambda/2$ to give $b(\mathbf{r})$. A consequence of this procedure is that the resolution of the reconstructed image is broadened by $\lambda/2$. Alternatively, the quality of the reconstructed image can be improved by combining holograms obtained at several different wavelengths.

For a single-point incoherent scatterer per unit cell, the above formulation will reconstruct the coherent scattering length with the incoherent scatterer located at the origin. For a uniformly random distribution of point incoherent scatterers, the reconstruction origin will be the "center of illumination"—i.e., theoretically the center of the $|a(\mathbf{r})|^2$ distribution—which by definition occupies exactly the same volume as the sample.

VI. CONCLUSIONS

It has long been realized that the diffraction pattern from a monochromatic spherical-wave source can be inverted to give the three-dimensional structure of the scattering length distribution surrounding the source—a process known as "holography" or "Gabor holography." However, the mathematical formulations for atomic-resolution holography have been limited to samples with one *S*-wave source per unit cell. In this paper we have developed a kinematical formulation for the diffraction pattern of monochromatic plane waves from a distribution of coherent and incoherent scatterers. From this it is evident that one can reconstruct the atomic structure of samples with a uniformly random distribution of incoherent scatterers. We have also presented a formulation for holographic reconstruction that eliminates the twin-image problem from single-wavelength data.

Of consequence is that the present result demonstrates that the plane-wave diffraction pattern caused by random (and/or incoherent) elastic scatterers embedded within a periodic elastic scattering length distribution is analogous to that of spontaneous sources of isotropic radiation or spherical waves. This allows the reconstruction, to atomic resolution, of neutron holograms from materials rich in incoherent scatterers, such as hydrogen (e.g., biological or polymeric materials). This is possible as long as the total incoherent neutron scattering, predominantly arising from hydrogen atoms, is larger than the total coherent neutron scattering.

ACKNOWLEDGMENT

The authors would like to thank Thad Harroun for his careful reading of the manuscript and the debugging of the Latex file.

APPENDIX A: DIFFRACTION PATTERN OF A SINGLE-POINT SOURCE

Consider a single-point source of monochromatic spherical waves, with displacement length amplitude a located at the origin of the real-space coordinate system. Suppressing the time dependence, the unperturbed source or reference-wave displacement at a detector, located at $\mathbf{R}$ is thus

$$\psi_{ref}(\mathbf{R}) = a\frac{e^{ik|\mathbf{R}|}}{|\mathbf{R}|}. \tag{A1}$$

This expression for the reference wave is independent of the direction of the detector, $\hat{\mathbf{R}}$.

The scattered or object wave at the detector, resulting from the source wave interacting with an object scattering length density, $b(\mathbf{r}_0)$, can be written as

$$\begin{aligned}\psi_{obj}(\mathbf{R}) &= \int \psi_{ref}(\mathbf{r}_0)b(\mathbf{r}_0)\frac{e^{ik(|\mathbf{R}-\mathbf{r}_0|)}}{|\mathbf{R}-\mathbf{r}_0|}\mathrm{d}\mathbf{r}_0 \\ &= ae^{ik|\mathbf{R}|}\int \frac{b(\mathbf{r}_0)e^{ik(|\mathbf{r}_0|+|\mathbf{R}-\mathbf{r}_0|-|\mathbf{R}|)}}{|\mathbf{r}_0||\mathbf{R}-\mathbf{r}_0|}\mathrm{d}\mathbf{r}_0. \end{aligned}\tag{A2}$$

For a detector in the far field $|\mathbf{R}| \gg \mathbf{r}_0$, the wave vector in the direction of the detector is defined as $\mathbf{k}_{out} = k\hat{\mathbf{R}}$. In this case, the path lengths in the above expressions can be approximated as $|\mathbf{R}-\mathbf{r}_0| \cong |\mathbf{R}|$, and $k(|\mathbf{R}-\mathbf{r}_0|-|\mathbf{R}|) \cong -\mathbf{k}_{out}\cdot\mathbf{r}_0$. Thus, in the far field, the expression for the object wave at the detector becomes

$$\psi_{obj}(\mathbf{R}) \cong a\frac{e^{ikR}}{R}\int \frac{b(\mathbf{r}_0)e^{i(kr_0-\mathbf{k}_{out}\cdot\mathbf{r}_0)}}{|\mathbf{r}_0|}\mathrm{d}\mathbf{r}_0 \equiv \psi_{obj}(\mathbf{k}_{out}). \tag{A3}$$

By substituting a reciprocal relationship for the object scattering length density, defined by

$$b(\mathbf{r}_0) = \frac{1}{\sqrt{(2\pi)^3}}\int B(\mathbf{q})e^{i\mathbf{q}\cdot\mathbf{r}_0}\mathrm{d}\mathbf{q}, \tag{A4}$$

the object wave at the detector can be expressed as

$$\begin{aligned}\psi_{obj}(\mathbf{k}_{out}) &= a\frac{e^{ikR}}{R}\frac{1}{\sqrt{(2\pi)^3}}\int\int \frac{B(\mathbf{q})e^{i[kr_0-(\mathbf{k}_{out}-\mathbf{q})\cdot\mathbf{r}_0]}}{|\mathbf{r}_0|}\mathrm{d}\mathbf{r}_0\mathrm{d}\mathbf{q} \\ &= a\frac{e^{ikR}}{R}\frac{4\pi}{\sqrt{(2\pi)^3}}\int \frac{B(\mathbf{q})}{|\mathbf{q}|^2-2\mathbf{k}_{out}\cdot\mathbf{q}}\mathrm{d}\mathbf{q} \equiv a\frac{e^{ikR}}{R}\chi(\mathbf{k}_{out}). \end{aligned}\tag{A5}$$

As defined above, $\chi(\mathbf{k}_{out})$ is a multiplicative factor which expresses the directional modulation of the source wave, caused by the object.

The three terms in the expression for the detected intensity can be written as follows: The intensity of the unperturbed source or reference wave is given by

$$I_R(\mathbf{k}_{out}) \equiv \psi^*_{ref}(\mathbf{R})\psi_{ref}(\mathbf{R}) \cong \frac{a*a}{R^2}. \tag{A6}$$

The intensity from the interference between the reference and object waves,

$$\begin{aligned}I_H(\mathbf{k}_{out}) &\equiv \psi^*_{ref}(\mathbf{R})\psi_{obj}(\mathbf{R}) + \text{c.c.} \\ &\cong \frac{a*a}{R^2}\int \frac{b(\mathbf{r}_0)e^{i(kr_0-\mathbf{k}_{out}\cdot\mathbf{r}_0)}}{|\mathbf{r}_0|}\mathrm{d}\mathbf{r}_0 + \text{c.c.} \\ &\equiv I_R(\mathbf{k}_{out})2\,\mathrm{Re}[\chi(\mathbf{k}_{out})]. \end{aligned}\tag{A7}$$

The object self-interference intensity

$$\begin{aligned}I_O(\mathbf{k}_{out}) &\equiv \psi^*_{obj}(\mathbf{R})\psi_{obj}(\mathbf{R}) \cong \frac{a*a}{R^2}\left|\int \frac{b(\mathbf{r}_0)e^{i(kr_0-\mathbf{k}_{out}\cdot\mathbf{r}_0)}}{|\mathbf{r}_0|}\mathrm{d}\mathbf{r}_0\right|^2 \\ &\equiv I_R(\mathbf{k}_{out}) \times |\chi(\mathbf{k}_{out})|^2. \end{aligned}\tag{A8}$$

The three terms are combined and written in terms of the experimentally observable directional modulation factor $\chi(\mathbf{k}_{out})$ in Eqs. (3) and (4).

APPENDIX B: DIFFRACTION PATTERN OF A CONTINUOUS SOURCE DISTRIBUTION

An extended source in real space can be described by the continuous complex amplitude density $a(\mathbf{r}_s)$. By writing the phase as a continuous function, it is implied that the phases

of the source displacement at different real-space points have a common origin in time; in other words, such a source is a "coherent" source. In this case, the reference wave at the detector location, **R**, is

$$\psi_{ref}(\mathbf{R}) = \int \frac{a(\mathbf{r}_s)e^{ik|\mathbf{R}-\mathbf{r}_s|}}{|\mathbf{R}-\mathbf{r}_s|}\mathrm{d}\mathbf{r}_s \cong \frac{e^{ikR}}{R}\int a(\mathbf{r}_s)e^{-i\mathbf{k}_{out}\cdot\mathbf{r}_s}\mathrm{d}\mathbf{r}_s \equiv \psi_{ref}(\mathbf{k}_{out}), \tag{B1}$$

where the second half of the above expression is an approximation for a detector in the far field. Again, in the far field, the outgoing wave vector $\mathbf{k}_{out}=k\hat{\mathbf{R}}$. The object wave at the detector in the far field becomes

$$\psi_{obj}(\mathbf{R}) \cong \frac{e^{ikR}}{R}\int\int \frac{a(\mathbf{r}_s)b(\mathbf{r}_0)e^{ik|\mathbf{r}_0-\mathbf{r}_s|}}{|\mathbf{r}_0-\mathbf{r}_s|}e^{-i\mathbf{k}\cdot\mathbf{r}_0}\mathrm{d}\mathbf{r}_0\mathrm{d}\mathbf{r}_s \equiv \psi_{obj}(\mathbf{k}_{out}). \tag{B2}$$

By defining a reciprocal-space relationship for $a(\mathbf{r}_s)$, similar to the one already defined for $b(\mathbf{r}_0)$, namely,

$$a(\mathbf{r}_s) = \frac{1}{\sqrt{(2\pi)^3}}\int A(\mathbf{q})e^{i\mathbf{q}\cdot\mathbf{r}_s}\mathrm{d}\mathbf{q}, \tag{B3}$$

it is straightforward to derive

$$\psi_{obj}(\mathbf{k}_{out}) = \frac{e^{ikR}}{R}\frac{4\pi}{\sqrt{(2\pi)^3}}\int \frac{A(\mathbf{k}_{out}-\mathbf{q})B(\mathbf{q})}{|\mathbf{q}|^2-2\mathbf{k}_{out}\cdot\mathbf{q}}\mathrm{d}\mathbf{q}. \tag{B4}$$

Equations (9) and (10) follow by evaluating the three terms, $\psi^*_{ref}\psi_{ref}$, $(\psi^*_{ref}\psi_{obj}+\text{c.c.})$, and $\psi^*_{obj}\psi_{obj}$, using the above expressions.

APPENDIX C: DIFFRACTION PATTERN OF A SET OF INDEPENDENT SOURCES

Appendix A gives expressions of the diffraction pattern for a single-point source, and Appendix B generalizes the expressions to the case of an extended, continuous, or coherent source. This appendix tackles the problem of generalized "independent" sources. Here "independent" or "incoherent" sources are represented by a set of identical sources, which are uncorrelated in time—i.e., whose relative phases do not have a common origin in time—and are therefore random. This necessitates the expression of intensities by an "ensemble average" of the waves from the set of independent, uncorrelated sources.

The notation in this appendix follows the notation developed earlier. The source- or reference-wave displacement for a detector located at **R**, in the far field, for a member of the set of uncorrelated or incoherent sources is expressed as

$$\psi_{ref\_n}(\mathbf{R}) \cong \psi_{ref\_n}(\mathbf{k}_{out}) = \frac{e^{ikR}}{R}\int a(\mathbf{r}_s)e^{-i(\mathbf{k}_{out}\cdot\mathbf{r}_s+\phi_n)}\mathrm{d}\mathbf{r}_s. \tag{C1}$$

Here, the ensemble is the set of source waves whose members are denoted by the index n, with random relative phases, ϕ_n. In the context of a kinematical theory, the role of the phase ϕ_n is to provide a random spatial displacement for every member of the source-wave ensemble. With this understanding and with a view to making the notation concise, the explicit reference to ϕ_n can be dropped by explicitly writing a real-space variable $\mathbf{r}_{sn}$ for each member of the ensemble with index n. The source wave for ensemble member n is rewritten as

$$\psi_{ref\_n}(\mathbf{k}_{out}) = \frac{e^{ikR}}{R}\int a(\mathbf{r}_{sn})e^{-i\mathbf{k}_{out}\cdot\mathbf{r}_{sn}}\mathrm{d}\mathbf{r}_{sn}, \tag{C2}$$

and the object wave from this representative member is expressed as

$$\psi_{obj\_n}(\mathbf{k}_{out}) = \frac{e^{ikR}}{R}\int\int \frac{a(\mathbf{r}_{sn})b(\mathbf{r}_0)e^{ik|\mathbf{r}_0-\mathbf{r}_{sn}|}}{|\mathbf{r}_0-\mathbf{r}_{sn}|}e^{-i\mathbf{k}_{out}\cdot\mathbf{r}_0}\mathrm{d}\mathbf{r}_0\mathrm{d}\mathbf{r}_{sn}. \tag{C3}$$

The reference-wave intensity is

$$\begin{aligned} I_R(\mathbf{k}_{out}) &= \langle\psi^*_{ref}(\mathbf{k}_{out})\psi_{ref}(\mathbf{k}_{out})\rangle_{ensemble} = \left\langle\int\int \frac{a^*(\mathbf{r}_{s1})a(\mathbf{r}_{s2})}{R^2}e^{-i\mathbf{k}_{out}\cdot(\mathbf{r}_{s2}-\mathbf{r}_{s1})}\mathrm{d}\mathbf{r}_{s1}\mathrm{d}\mathbf{r}_{s2}\right\rangle \\ &= \left\langle\int\int_{\mathbf{r}_{s1}\neq\mathbf{r}_{s2}} \frac{a^*(\mathbf{r}_{s1})a(\mathbf{r}_{s2})}{R^2}e^{-i\mathbf{k}_{out}\cdot(\mathbf{r}_{s2}-\mathbf{r}_{s1})}\mathrm{d}\mathbf{r}_{s1}\mathrm{d}\mathbf{r}_{s2}\right\rangle + \left\langle\int\int \frac{a^*(\mathbf{r}_{s1})a(\mathbf{r}_{s2})}{R^2}e^{-i\mathbf{k}_{out}\cdot(\mathbf{r}_{s2}-\mathbf{r}_{s1})}\delta(\mathbf{r}_{s1}-\mathbf{r}_{s2})\mathrm{d}\mathbf{r}_{s1}\mathrm{d}\mathbf{r}_{s2}\right\rangle \\ &= \frac{1}{R^2}\int |a(\mathbf{r}_s)|^2\mathrm{d}\mathbf{r}_s. \end{aligned} \tag{C4}$$

In the above derivation, the ensemble average is subdivided into two terms: one containing the product of displacements of any two different members of the ensemble—i.e., the product of displacements of a typical member at different space points and the other containing the product of displacements at the same space point. The first term averages to zero under the stated assumption that the set of sources is completely uncorrelated. The second term is the squared magni-

tude of the displacement for a representative source.

Using the same argument, the interference between source and object wave gives a detected intensity

$$I_H(\mathbf{k}_{out}) = \langle \psi^*_{ref}(\mathbf{k}_{out})\psi_{obj}(\mathbf{k}_{out}) + \text{c.c.}\rangle_{ensemble} = \frac{1}{R^2}\int |a(\mathbf{r}_s)|^2 \left\{ \int \frac{b(\mathbf{r}_0)e^{ik|\mathbf{r}_0-\mathbf{r}_s|}}{|\mathbf{r}_0-\mathbf{r}_s|} e^{-i\mathbf{k}_{out}\cdot\mathbf{r}_0} d\mathbf{r}_0 \right\} \times e^{i\mathbf{k}_{out}\cdot\mathbf{r}_s} d\mathbf{r}_s + \text{c.c.} \quad \text{(C5)}$$

and the self-interference of the object wave produces the detected intensity

$$I_O(\mathbf{k}_{out}) = \langle \psi^*_{obj}(\mathbf{k}_{out})\psi_{obj}(\mathbf{k}_{out})\rangle_{ensemble} = \frac{1}{R^2}\int |a(\mathbf{r}_s)|^2 \left| \int \frac{b(\mathbf{r}_0)e^{ik|\mathbf{r}_0-\mathbf{r}_s|}}{|\mathbf{r}_0-\mathbf{r}_s|} e^{-i\mathbf{k}_{out}\cdot\mathbf{r}_0} d\mathbf{r}_0 \right|^2 d\mathbf{r}_s. \quad \text{(C6)}$$

Equations (11)–(13) follow in a straightforward fashion by defining a reciprocal-space relationship for the squared magnitude of the source density:

$$A^2(\mathbf{q}) \equiv \frac{1}{\sqrt{(2\pi)^3}} \int |a(\mathbf{r}_s)|^2 e^{-i\mathbf{q}\cdot\mathbf{r}_s} d\mathbf{r}_s. \quad \text{(C7)}$$

APPENDIX D: DIFFRACTION PATTERN FROM COHERENT AND INCOHERENT SCATTERERS

Expressions for the diffraction patterns from spontaneous coherent and incoherent sources of monochromatic spherical waves are given in Appendixes A–C. For atomic structure holography using electromagnetic radiation, it is possible to approximate spontaneous monochromatic spherical-wave sources inside an atomic structure—e.g., by atoms undergoing x-ray fluorescence or photoelectron emission. For thermal neutrons, there are no known cases of spontaneous atomic sources emitting monochromatic thermal neutrons. In a thermal neutron scattering experiment, monochromatic plane waves are typically obtained by a Bragg reflection of a "white beam" from a known set of planes of a crystal placed far from the sample. These neutron plane waves are incident on a sample, or object, inside which they are scattered primarily by atomic nuclei and detected by a scattered-wave detector (or, simply, "detector"). The scattering from the object can be separated into coherent and incoherent components. In the kinematical context—i.e., when purely elastic scattering from the entire object is assumed—an atomic structure that is invariant under translation—an atomic lattice—gives "coherent" scattering. Any random irregularity in the translational order of the object atomic structure gives rise to "incoherent" scattering. Effects that give rise to incoherent thermal neutron scattering include random variations of scattering lengths at lattice sites because of nuclear spin (spin incoherence), random variations of scattering length at lattice sites because of isotopic substitutions (isotope incoherence), or in general, any random translational disorder such as solute atoms in random interstitial sites or oriented grains or crystallites at random relative locations. Although such incoherent scattering is not associated with individual atomic sites or "sources," one can nevertheless, in a collective sense, differentiate between the "coherent" (associated with perfect translational order) and the "incoherent" (associated with randomness) scattering lengths at space points. Turning points in the coherent scattering length distribution are then identified as lattice sites which contain atoms.

This appendix develops a second-order kinematical theory of plane-wave scattering from a distribution of spherical-wave scatterers whose structure includes coherent and incoherent components. Results and notations developed in Appendixes A–C are used. In particular, the device of "ensemble averages," as introduced in Appendix C, is used to evaluate detected intensities. Individual members of the ensemble are conceptually identified by random differences in the scattering length distribution. These random differences produce incoherent scattering. The coherent scattering length distribution is conceptually the same for all members of the ensemble. The object scattering-length density is written as a sum of coherent (subscript c) and incoherent (subscript i) components:

$$b(\mathbf{r}_0) = b_c(\mathbf{r}_0) + b_i(\mathbf{r}_0), \quad \text{(D1)}$$

where it is understood that the incoherent component $b_i(\mathbf{r}_0)$ *will be treated in the same manner* as the incoherent source distribution of Appendix C.

Consider a monochromatic plane wave with wave number k and wave vector $\mathbf{k}_{in}$ incident on the object. The displacement from this incident wave, at any point, $\mathbf{r}$, in the object coordinate system is

$$\psi_{inc}(\mathbf{r}) = Ce^{i\mathbf{k}_{in}\cdot\mathbf{r}}. \quad \text{(D2)}$$

The incident wave does not interact directly with the scattered-wave detector. The squared amplitude of the incident wave, $|C|^2$, is usually estimated by ancillary detectors and used for normalization of the scattered-wave detected intensity.

The scattered-wave detector located at $\mathbf{R}$ is in the far field of the object with the corresponding outgoing wave vector, $\mathbf{k}_{out} \equiv k\hat{\mathbf{R}}$. The first-order scattered wave ψ_I is caused by the direct interaction of the incident plane wave with the object scattering length distribution. The first-order scattered wave at the detector is

$$\psi_I(\mathbf{R}) = \int \psi_{inc}(\mathbf{r}_0)\frac{b(\mathbf{r}_0)e^{ik|\mathbf{R}-\mathbf{r}_0|}}{|\mathbf{R}-\mathbf{r}_0|} d\mathbf{r}_0 \cong C\frac{e^{ikR}}{R}\int b(\mathbf{r}_0)e^{-i(\mathbf{k}_{out}-\mathbf{k}_{in})\cdot\mathbf{r}_0} d\mathbf{r}_0 \equiv \psi_I(\mathbf{k}_{in},\mathbf{k}_{out}). \quad \text{(D3)}$$

The first-order scattered wave (produced at point $\mathbf{r}_{01}$) rescatters inside the object (at point $\mathbf{r}_{02}$) to produce a second-order scattered wave. Thus, the second-order scattered wave at the detector can be written as

$$\psi_{II}(\mathbf{R}) = \int \psi_I(\mathbf{r}_{02}) \frac{b(\mathbf{r}_{02}) e^{ik|\mathbf{R}-\mathbf{r}_{02}|}}{|\mathbf{R}-\mathbf{r}_{02}|} \mathrm{d}\mathbf{r}_{02} \cong C \frac{e^{ikR}}{R} \int \int_{\mathbf{r}_{01} \neq \mathbf{r}_{02}} b(\mathbf{r}_{01}) b(\mathbf{r}_{02}) \frac{e^{ik|\mathbf{r}_{02}-\mathbf{r}_{01}|}}{|\mathbf{r}_{02}-\mathbf{r}_{01}|} e^{-i(\mathbf{k}_{out}\cdot\mathbf{r}_{02} - \mathbf{k}_{in}\cdot\mathbf{r}_{01})} \mathrm{d}\mathbf{r}_{01} \mathrm{d}\mathbf{r}_{02} \equiv \psi_{II}(\mathbf{k}_{in}, \mathbf{k}_{out}). \tag{D4}$$

Note that to avoid double counting, points $\mathbf{r}_{01}$ and $\mathbf{r}_{02}$ are not allowed to coincide.

The total intensity at the detector is given by $\langle \psi_I^* \psi_I + 2\,\mathrm{Re}(\psi_I^* \psi_{II}) + \psi_{II}^* \psi_{II} \rangle_{\text{ensemble}}$. These three terms are evaluated below.

The detected intensity from first-order scattering (Born approximation) is

$$I_I(\mathbf{k}_{in}, \mathbf{k}_{out}) = \langle \psi_I^*(\mathbf{k}_{in}, \mathbf{k}_{out}) \psi_I(\mathbf{k}_{in}, \mathbf{k}_{out}) \rangle = \left\langle \frac{C^2}{R^2} \int \int b^*(\mathbf{r}_{01}) b(\mathbf{r}_{02}) e^{-i(\mathbf{k}_{out}-\mathbf{k}_{in})\cdot(\mathbf{r}_{02}-\mathbf{r}_{01})} \mathrm{d}\mathbf{r}_{01} \mathrm{d}\mathbf{r}_{02} \right\rangle. \tag{D5}$$

To take the ensemble average, the product of scattering length densities is explicitly expanded into products of the coherent and incoherent components. Using the abbreviated notation $b(\mathbf{r}_{01}) = b_c(\mathbf{r}_{01}) + b_i(\mathbf{r}_{01}) \equiv c1 + i1$, etc., where $c1$ and $i1$ are the coherent and incoherent components, respectively, of $b(\mathbf{r})$ at point $\mathbf{r}_{01}$,

$$b^*(\mathbf{r}_{01}) b(\mathbf{r}_{02}) = (c1 + i1)^*(c2 + i2) = \{c1^* c2 + i1^* i2 + i1^* c2 + c1^* i2\}. \tag{D6}$$

Note that products of coherent terms such as $c1^* c2$ can be integrated and averaged over all space; the integrals of products of coherent and incoherent terms such as $c1^* i2$ average to zero because there is no spatial correlation between the coherent and incoherent distributions; and terms containing products of incoherent terms such as $i1^* i2$ have to be integrated with an implicit $\delta(\mathbf{r}_{01} - \mathbf{r}_{02})$, because they are not correlated at different space points. The line of reasoning is similar to that taken for evaluating ensemble averages from incoherent sources in Appendix C. This results in

$$\begin{aligned} I_I(\mathbf{k}_{in}, \mathbf{k}_{out}) &= \frac{C^2}{R^2} \left(\int \int b_c^*(\mathbf{r}_{01}) b_c(\mathbf{r}_{02}) e^{-i(\mathbf{k}_{out}-\mathbf{k}_{in})\cdot(\mathbf{r}_{02}-\mathbf{r}_{01})} \mathrm{d}\mathbf{r}_{01} \mathrm{d}\mathbf{r}_{02} + \int \int b_i^*(\mathbf{r}_{01}) b_i(\mathbf{r}_{02}) e^{-i(\mathbf{k}_{out}-\mathbf{k}_{in})\cdot(\mathbf{r}_{02}-\mathbf{r}_{01})} \delta(\mathbf{r}_{01} - \mathbf{r}_{02}) \mathrm{d}\mathbf{r}_{01} \mathrm{d}\mathbf{r}_{02} \right) \\ &= \frac{C^2}{R^2} \left(\left| \int b_c(\mathbf{r}) e^{-i(\mathbf{k}_{out}-\mathbf{k}_{in})\cdot\mathbf{r}} \mathrm{d}\mathbf{r} \right|^2 + \int |b_i(\mathbf{r})|^2 e^{-i(\mathbf{k}_{out}-\mathbf{k}_{in})\cdot\mathbf{r}} \mathrm{d}\mathbf{r} \right), \end{aligned} \tag{D7}$$

where the δ has been used to integrate over one of the two variables in the expression for the incoherent intensity.

The first-order scattered-wave-detected intensity thus contains two terms—the first term is caused entirely by the coherent scattering length distribution, while the second term is the intensity from the incoherent scattering length distribution. If the incoherent scattering length distribution is uniformly random over all space, then the second term is a constant, independent of direction.

To put this concisely, we define a change in wave vector, $\kappa = \mathbf{k}_{out} - \mathbf{k}_{in}$, and reciprocal-space relationships for the coherent scattering length density and squared magnitude of the incoherent scattering length density:

$$B_c(\mathbf{q}) = \frac{1}{\sqrt{(2\pi)^3}} \int b_c(\mathbf{r}_0) e^{-i\mathbf{q}\cdot\mathbf{r}_0} \mathrm{d}\mathbf{r}_0 \tag{D8}$$

and

$$B_i^2(\mathbf{q}) = \frac{1}{\sqrt{(2\pi)^3}} \int |b_i(\mathbf{r}_0)|^2 e^{-i\mathbf{q}\cdot\mathbf{r}_0} \mathrm{d}\mathbf{r}_0. \tag{D9}$$

By appropriate normalization to the incident-wave intensity, the detected intensity from first-order scattering is readily seen to be proportional to

$$I_I(\mathbf{k}_{in}, \mathbf{k}_{out}) = \frac{1}{R^2} [B_c^*(\boldsymbol{\kappa}) B_c(\boldsymbol{\kappa}) + B_i^2(\boldsymbol{\kappa})]. \tag{D10}$$

This is the usual expression for plane-wave scattering in the Born approximation. If the coherent scattering length density is perfectly periodic in all three spatial dimensions, then it can be specified completely by a complex function at discrete points in reciprocal space. Intensity maxima (Bragg peaks) are observed when the changes in wave vector created by the experimental conditions coincide with the locations of these discrete points in reciprocal space. For experimentally accessible changes in wave vector that do not correspond to the periodic lattice of reciprocal-space points, one observes a

continuous intensity given by the incoherent scattering term. In the kinematical context, this term will be a constant for a *uniformly* random distribution of scatterers. Usually, a variation in this intensity as a function of change in wave vector is associated with dynamical effects—i.e., movement of the "scatterers"—and generally classified as the Debye-Waller factor. In the kinematical context, any nonuniformly random component of scattering length will cause such a variation.

The detected intensity of the interference between the first- and second-order scattered waves is

$$I_H(\mathbf{k}_{in},\mathbf{k}_{out}) = \langle \psi_I^*(\mathbf{k}_{in},\mathbf{k}_{out})\psi_{II}(\mathbf{k}_{in},\mathbf{k}_{out})\rangle + \text{c.c.}$$
$$= \left\langle \frac{C^2}{R^2}\int_{\mathbf{r}_{01}}\int\int_{\mathbf{r}_{02}\neq\mathbf{r}_{03}} b^*(\mathbf{r}_{01})b(\mathbf{r}_{02})b(\mathbf{r}_{03})\frac{e^{ik|\mathbf{r}_{03}-\mathbf{r}_{02}|}}{|\mathbf{r}_{03}-\mathbf{r}_{02}|}e^{-i\{\mathbf{k}_{out}\cdot(\mathbf{r}_{03}-\mathbf{r}_{01})-\mathbf{k}_{in}\cdot(\mathbf{r}_{02}-\mathbf{r}_{01})\}}d\mathbf{r}_{01}d\mathbf{r}_{02}d\mathbf{r}_{03}\right\rangle + \text{c.c.} \quad \text{(D11)}$$

Once again, the ensemble average of the triple integral is evaluated by expanding the product of scattering length densities into products of coherent and incoherent components. Using the abbreviated notation defined previously, the terms in the product are

$$b^*(\mathbf{r}_{01})b(\mathbf{r}_{02})b(\mathbf{r}_{03}) = (c1+i1)^*(c2+i2)(c3+i3) = c1^*c2c3 + i1^*i2c3 + i1^*c2i3 + i1^*c2c3 + c1^*i2c3 + c1^*c2i3 + c1^*i2i3$$
$$+ i1^*i2i3. \quad \text{(D12)}$$

Only the first three terms above survive in the ensemble average of the triple integral. The remaining terms contain either an odd power of incoherent terms—which average to zero—or else contain products of incoherent terms at space points $\mathbf{r}_{02}$ and $\mathbf{r}_{03}$—which, as previously noted, are not allowed to coincide. Thus the ensemble average of these remaining terms becomes zero. The three surviving interference intensity terms are written out separately below.

The first of the three terms, $c1^*c2c3$, is readily identified as the intensity modulation of the first-order coherently scattered wave ($c1^*$) by the second-order wave produced by successive scattering from any two coherent scatterers ($c2$ and $c3$). By using the reciprocal-space expression for the coherent scattering length density to evaluate the triple integral, this intensity term is conveniently represented by the following expression (after normalization to the incident wave intensity $|C|^2$):

$$I_{H\_coh}(\mathbf{k}_{in},\mathbf{k}_{out}) = 2\,\text{Re}\left[\frac{4\pi}{R^2}B_c^*(\boldsymbol{\kappa})\int\frac{B_c(\mathbf{q})B_c(\boldsymbol{\kappa}-\mathbf{q})}{|\mathbf{q}|^2-2\mathbf{k}_{out}\cdot\mathbf{q}}d\mathbf{q}\right]$$
$$\equiv \frac{1}{R^2}2\,\text{Re}[B_c^*(\boldsymbol{\kappa})\tilde{B}_c(\boldsymbol{\kappa})]. \quad \text{(D13)}$$

The second term $i1^*i2c3$ is identified as the intensity modulation of a first-order incoherently scattered reference wave ($i1^*$) by a wave which is first scattered incoherently ($i2$) and then coherently ($c3$). It is thus analogous to the hologram modulation caused by "a distribution of independent inside sources" as expressed in Appendix C and in Eqs. (11)–(13). This intensity modulation term is a function of $\mathbf{k}_{out}$ only. It can be observed by fixing the incident beam direction in the object frame and measuring the scattered intensity in different directions with respect to the object. This mode of observation is often called "inside-source holography." Again, by using the reciprocal-space expressions for the coherent scattering length density and the squared magnitude of the incoherent scattering length distribution, this term is conveniently represented by

$$I_{H\_out}(\mathbf{k}_{out}) = 2\,\text{Re}\left[\frac{4\pi}{R^2}\int\frac{B_i^2(-\mathbf{q})B_c(\mathbf{q})}{|\mathbf{q}|^2-2\mathbf{k}_{out}\cdot\mathbf{q}}d\mathbf{q}\right]. \quad \text{(D14)}$$

The third term $i1^*i2i3$ is identified as the intensity modulation of a first-order incoherently scattered reference wave ($i1^*$) by a wave which is first scattered coherently ($c2$) and then incoherently ($i3$). This is the optically reciprocal case of the second term described above. This intensity modulation term is a function of $\mathbf{k}_{in}$ only. It can be observed by fixing the direction of the scattered-wave detector in the object frame and measuring the scattered intensity when a plane wave is incident on the object from different directions. This mode of observation is often called "inside-detector holography" because conceptually the coherent scattering occurs before the wave reaches the incoherent scatterer; hence, the incoherent scatterer acts as a detector. Using the reciprocal-space expressions for the coherent scattering length density and the squared magnitude of the incoherent scattering length distribution, this term is conveniently represented by

$$I_{H\_in}(\mathbf{k}_{in}) = 2\,\text{Re}\left[\frac{4\pi}{R^2}\int\frac{B_i^2(-\mathbf{q})B_c(\mathbf{q})}{|\mathbf{q}|^2-2(-\mathbf{k}_{in})\cdot\mathbf{q}}d\mathbf{q}\right]. \quad \text{(D15)}$$

The terms for the intensity from the self-interference of the second-order scattered wave, $\langle\psi_{II}^*\psi_{II}\rangle_{ensemble}$, can be evaluated by procedures similar to those outlined above.

It is now seen that the terms in all the expressions for detected intensity fall into two categories: ones that depend only on the coherent scattering length distribution [these are collected in Eqs. (15) and (16)] and ones that arise from the interaction of the incoherent and coherent scattering lengths

in the object. The "hologram intensity" terms [Eqs. (D14) and (D15)] from the interaction between incoherent and coherent scattering can be inverted, in certain situations, to give the coherent scattering length distribution. These situations are where it is possible to make simplifying assumptions about, or to infer, the incoherent scattering length distribution (i.e., where the incoherent scattering length distribution can be "deconvoluted" from the observations). The simplest two such cases are that (i) there is conceptually only one incoherent scatterer per period or "unit cell" of the object coherent scattering length density and (ii) there is a uniformly random distribution of incoherent scatterers in the object. It is possible, in a practical sense, to approximate the second situation with a large number of incoherent scatterers per unit cell.

APPENDIX E: ANALYTICAL SOLUTION TO *K*-LINE SHAPE

Here we present the detailed analytical solution for the shape of *K* lines when the "ideal" modulation function is convoluted with a generic Gaussian spread function. The intensity modulation for a point source diffraction pattern, given by Eq. (3), has two components. One component has a symmetric or quadratic dependence on $b(\mathbf{r})$—namely, $|\chi(\mathbf{k})|^2$—and thus contains no phase information. The other component is asymmetric or has a linear dependence on $b(\mathbf{r})$—namely, $2\mathrm{Re}[\chi(\mathbf{k})]$—and contains the phase information from which the scattering length distribution can be reconstructed. Convoluting a symmetric spread function with the above-mentioned functions results in the asymmetric component having a much reduced amplitude, much more so than the amplitude of the symmetric component. This is because near the center of the pattern, the two halves of the asymmetric pattern cancel each other out. The issue then is one of practicality—how broad a convolution function can one afford to employ before the phase information is, for all practical purposes, lost. It turns out that a numerical evaluation of this effect is difficult because of the cancellation of large numbers leading to significant truncation errors.

The "ideal" *K*-line modulation function due to a point at $\mathbf{q}_0$ in reciprocal space is given by substituting a delta function $bc[\delta(\mathbf{q}-\mathbf{q}_0)]/V_{cell}$, where b is the scattering length, c is the complex nondimensional amplitude factor, and V_{cell} is the volume of the primitive cell, for $B(\mathbf{q})$ in Eq. (6). For a periodic scattering length distribution, as given in Eq. (7), each term in Eq. (8) would be treated in the same manner as a point at $\mathbf{q}_0=\boldsymbol{\tau}_{hkl}$.

For a nonideal case, $B(\mathbf{q})$ can be considered as some averaging function. Here consider a Gaussian where

$$B(\mathbf{q}) = \frac{bc}{V_{cell}}\left(\frac{\mu}{\pi}\right)^{3/2} e^{(-\mu|\mathbf{q}-\mathbf{q}_0|^2)}. \tag{E1}$$

Equation (6) is evaluated at all values of μ and can be rewritten as

$$\chi(\mathbf{k}) = \frac{bc}{V_{cell}}\int \frac{B(\mathbf{q})}{|\mathbf{q}|^2 - 2\mathbf{k}\cdot\mathbf{q}} d^3\mathbf{q} = \frac{bc}{V_{cell}}\int \frac{B(\mathbf{q})}{|\mathbf{q}-\mathbf{k}|^2 - |\mathbf{k}|^2} d^3\mathbf{q}. \tag{E2}$$

Equation (E2) is rewritten using the change of variable $\mathbf{u}=\mathbf{q}_0-\mathbf{k}$, $\mathbf{t}=\mathbf{q}-\mathbf{k}$ as follows:

$$\chi(\mathbf{k}) = \frac{bc}{V_{cell}}\left(\frac{\mu}{\pi}\right)^{3/2}\int \frac{e^{(-\mu|\mathbf{t}-\mathbf{u}|^2)}}{|\mathbf{t}|^2 - |\mathbf{k}|^2} d^3\mathbf{t}. \tag{E3}$$

Rewriting Eq. (E3) in polar coordinates we get

$$\chi(\mathbf{k}) = \frac{bc}{uV_{cell}}\left(\frac{\mu}{\pi}\right)^{1/2}\int_0^\infty dt\int_0^\pi \sin\theta\, d\theta \frac{e^{[-\mu(t^2-2ut\cos\theta+u^2)]}}{t^2-k^2} t^2. \tag{E4}$$

Changing the angular variable θ to $x=\cos\theta$ and integrating over x we rewrite Eq. (E4) as follows:

$$\chi(\mathbf{k}) = \frac{bc}{uV_{cell}}\left(\frac{\mu}{\pi}\right)^{1/2}\int_0^\infty \frac{e^{[-\mu(t-u)^2]} - e^{[-\mu(t+u)^2]}}{t^2-k^2} t\, dt, \tag{E5}$$

resulting in

$$\chi(\mathbf{k}) = \frac{bc}{uV_{cell}}\left(\frac{\mu}{\pi}\right)^{1/2}\int_{-\infty}^\infty \frac{te^{[-\mu(t-u)^2]}}{t^2-k^2} dt. \tag{E6}$$

It should be noted that all integrals shown above are defined in terms of principal value. Expressing the fractional part of Eq. (E6) in terms of

$$\frac{t}{t^2-k^2} = \frac{1}{2}\left(\frac{1}{t-k} + \frac{1}{t+k}\right), \tag{E7}$$

the integral for $\chi(\mathbf{k})$ can then be expressed as a sum of two terms. The first term is written as

$$\chi_1(\mathbf{k}) = \frac{bc}{2uV_{cell}}\left(\frac{\mu}{\pi}\right)^{1/2}\int_{-\infty}^\infty \frac{te^{[-\mu(t-u)^2]}}{t-k} dt, \tag{E8}$$

while the second term is expressed as

$$\chi_2(\mathbf{k}) = \frac{bc}{2uV_{cell}}\left(\frac{\mu}{\pi}\right)^{1/2}\int_{-\infty}^\infty \frac{te^{[-\mu(t-u)^2]}}{t+k} dt. \tag{E9}$$

The two terms of the $\chi(\mathbf{k})$ integral are analogous. Changing the variables $t-u=z$ and $z^*=\mu^{1/2}z$, we then get

$$\chi_1(\mathbf{k}) = \frac{bc}{2uV_{cell}}\left(\frac{\mu}{\pi}\right)^{1/2}\int_{-\infty}^\infty \frac{e^{-\mu z^2}}{z+u-k} dz$$
$$= \frac{bc}{2uV_{cell}}\left(\frac{\mu}{\pi}\right)^{1/2}\int_{-\infty}^\infty \frac{e^{-z^2}}{z+\mu^{1/2}(u-k)} dz \tag{E10}$$

and

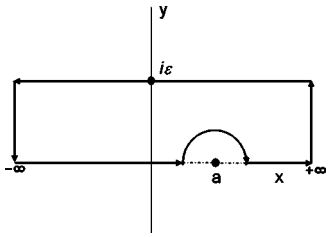

FIG. 2. Schematic representation of the integral in Eq. (E12) in the complex plane $z=x+iy$.

$$\chi_2(\mathbf{k}) = \frac{bc}{2uV_{cell}}\left(\frac{\mu}{\pi}\right)^{1/2}\int_{-\infty}^{\infty}\frac{e^{-\mu z^2}}{z+u+k}dz$$

$$= \frac{bc}{2uV_{cell}}\left(\frac{\mu}{\pi}\right)^{1/2}\int_{-\infty}^{\infty}\frac{e^{-z^2}}{z+\mu^{1/2}(u+k)}dz. \quad \text{(E11)}$$

These two integrals [Eqs. (E10) and (E11)] are computed in terms of the principal value and are particular cases of the following principal value integral

$$f(a) = \int_{-\infty}^{\infty}\frac{e^{-z^2}}{a-z}dz, \quad \text{(E12)}$$

where a is real.

Figure 2 schematically shows the evaluation of Eq. (E12). Referring to Fig. 2 and integrating in the upper part of the complex plane yields

$$-\frac{\pi}{i}w(a) = -\frac{\pi}{i}e^{-a^2}\left(1+\frac{2i}{\sqrt{\pi}}\int_0^a e^{t^2}dt\right). \quad \text{(E13)}$$

The two parts at $\pm\infty$ give rise to a value of 0, while the lower dashed arrow yields $f(a)$. The semicircle around point A corresponds to a value of $-i\pi e^{-a^2}$.

From the real part of the zero we then obtain the expression

$$f(a) = \int_{-\infty}^{\infty}\frac{e^{-z^2}}{a-z}dz = 2\sqrt{\pi}e^{-a^2}\int_0^a e^{y^2}dy. \quad \text{(E14)}$$

We then get

$$\chi(\mathbf{k}) = \frac{bc}{2uV_{cell}}\sqrt{\frac{\mu}{\pi}}2\sqrt{\pi}\left[e^{-\mu(u-k)^2}\int_0^{\sqrt{\mu}(u-k)}e^{y^2}dy + e^{-\mu(u+k)^2}\int_0^{\sqrt{\mu}(u+k)}e^{y^2}dy\right], \quad \text{(E15)}$$

which then simplifies to the following:

$$\chi(\mathbf{k}) = \frac{bc}{uV_{cell}}\sqrt{\mu}\left[e^{-\mu(u-k)^2}\int_0^{\sqrt{\mu}(u-k)}e^{y^2}dy + e^{-\mu(u+k)^2}\int_0^{\sqrt{\mu}(u+k)}e^{y^2}dy\right]. \quad \text{(E16)}$$

The above expression [Eq. (E16)] is the exact solution to K-line shapes. The solution is expressed in terms of the Dawson integral which we derive below in order to facilitate its numerical evaluation.

A sample calculation of the K-line profile for a range of assumed Gaussian widths is shown in Fig. 3. A practical limit for experimental observation is given by

$$\frac{q_0}{2}\sqrt{\mu} \geqslant 1;$$

that is, the maxima of the Dawson integral for each q does not fall on the minima of successive q.

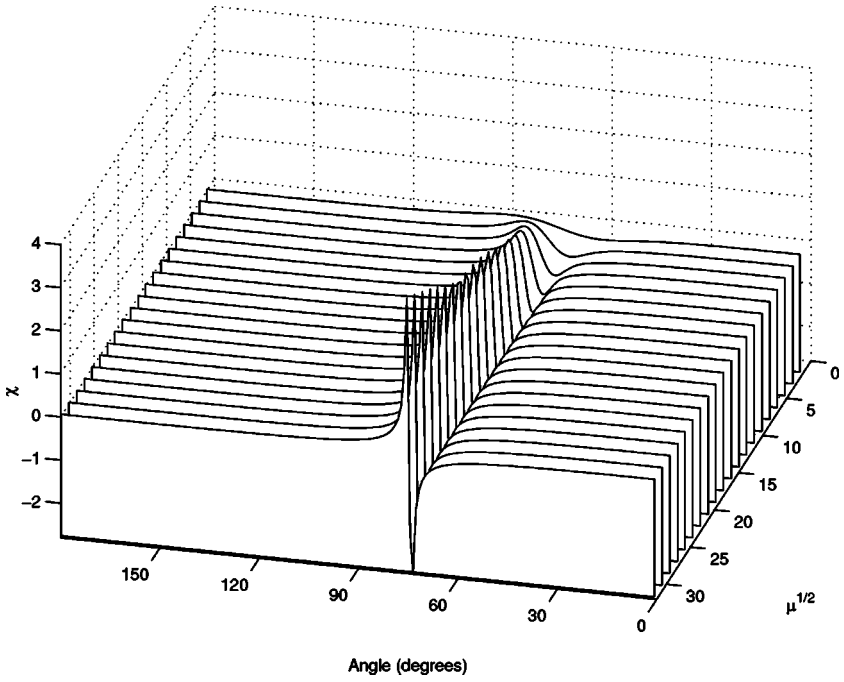

FIG. 3. Calculation of the modulation function χ, for $k=2\pi/1.3$ Å, $q_0=2(2\pi/5)$ Å and $\mu^{1/2}$ from 0 to 30. The factor bc/V_{cell} is not included.

APPENDIX F: CALCULATION OF THE DAWSON INTEGRAL

The Dawson integral can be written as follows:

$$e^{-y^2}\int_0^y e^{t^2}dt. \tag{F1}$$

For small values of y we can carry out a serial expansion of the integral and obtain the following:

$$ye^{-y^2}\sum_{k=0}^{\infty}\frac{y^{2k}}{(2k+1)k!}. \tag{F2}$$

The above form of the integral works well for values of $y<4$. For larger values of y we can rewrite the integral as follows:

$$e^{-y^2}\int_0^y e^{x^2}dx = \int_0^y e^{(x^2-y^2)}dx. \tag{F3}$$

Letting $t=y-x$ we can rewrite Eq. (F3) as follows:

$$\int_0^y e^{(-2ty+t^2)}dt. \tag{F4}$$

To perform the expansion of Eq. (F4) we let $s=2ty$ and obtain the following:

$$\frac{1}{2y}\int_0^{2y^2} e^{-s}e^{s^2/4y^2}ds. \tag{F5}$$

When $2y^2$ is large (~ 30 when $y>4$) we can use a Gauss-Laguerre numerical integration with three points to compute the integral given by Eq. (F5). The limit between large y and small y was empirically established to be $y=4$.

[1] B. Sur, R. B. Rogge, R. P. Hammond, V. N. P. Anghel, and J. Katsaras, Phys. Rev. Lett. **88**, 065505 (2002).
[2] G. L. Clark and W. Duane, Proc. Natl. Acad. Sci. U.S.A. **8**, 90 (1922).
[3] W. Kossel, V. Loeck, and H. Voges, Z. Phys. **94**, 139 (1935).
[4] S. Kikuchi, Jpn. J. Phys. **5**, 83 (1928).
[5] A. Szöke, in *Short Wavelength Coherent Radiation: Generation and Applications*, edited by T. Attwood and J. Boker, AIP Conf. Proc. No. 147 (AIP, New York, 1986).
[6] A. Szöke, Phys. Rev. B **47**, 14 044 (1993).
[7] T. Gog, P. M. Len, G. Materlik, D. Bahr, C. S. Fadley, and C. Sanchez-Hanke, Phys. Rev. Lett. **76**, 3132 (1996).
[8] D. Petrascheck, Phys. Rev. B **31**, R4043 (1985).
[9] S. W. Wilkins, Phys. Rev. Lett. **50**, 1862 (1983).
[10] W. L. Bragg, Nature (London) **149**, 470 (1942).
[11] D. Gabor, Nature (London) **161**, 777 (1948).
[12] G. R. Harp, D. K. Saldin, and B. P. Tonner, Phys. Rev. Lett. **65**, 1012 (1990).
[13] M. Zharnikov, M. Weinelt, P. Zebisch, M. Stichler, and H.-P. Steinrück, Phys. Rev. Lett. **73**, 3548 (1994).
[14] M. T. Sieger, J. M. Roesler, D.-S. Lin, T. Miller, and T.-C. Chiang, Phys. Rev. Lett. **73**, 3117 (1994).
[15] A. Orchowski, W. D. Rau, and H. Lichte, Phys. Rev. Lett. **74**, 399 (1995).
[16] M. Tegze and G. Faigel, Europhys. Lett. **16**, 41 (1991).
[17] M. Tegze and G. Faigel, Nature (London) **380**, 49 (1996).
[18] M. Tegze, G. Faigel, S. Marchesini, M. Belakhovsky, and A. I. Chumakov, Phys. Rev. Lett. **82**, 4847 (1999).
[19] S. G. Bompadre, T. W. Petersen, and L. B. Sorensen, Phys. Rev. Lett. **83**, 2741 (1999).
[20] B. Sur, R. B. Rogge, R. P. Hammond, V. N. P. Anghel, and J. Katsaras, Nature (London) **414**, 525 (2001).
[21] L. Cser, G. Török, G. Krexner, I. Sharkov, and B. Faragó, Phys. Rev. Lett. **89**, 175504 (2002).